CHAPTER IV

NON MEDIATED ELECTROCHEMICAL MEASUREMENT OF CYTOCHROME-C

COUPLED GOLD NANOPARTICLES

Introduction

Biology offers many examples of well-developed, efficient control over highly complex functions, specifically electron transfer. Of interest, is interfacing biological marcomolecules with well-defined nanomaterials, using bottom-up techniques, to control and mimic the inherent properties of the protein. There are examples of such interfaces in Photosystem I,[1] antibody based biosensors,[2,3] and biomolecular scaffolds.[4-6] By utilizing such specific proteins, they can be applied for novel functions, without the use of costly, difficult to synthesize materials.

One class of these proteins contains redox active centers in which a metal center transitions between charge states. Specifically, cytochrome-c (cyt-c) has been the subject of many studies and has well-known, characterized electron transfer behavior.[7-10] Cyt-c contains a redox active heme center that reversibly changes states between Fe^{+2}/Fe^{+3}. The water-soluble protein is located near cell mitocondria, and plays a critical step in the electron transport chain by transferring an electron from complex III (cytochrome-bc$_1$) to complex IV (cytochrome-c oxidase). Because of its highly reversible behavior, cyt-c has become the center of many electron transfer studies.

Eddowes and Hill first showed in 1977 that cyt-c exhibits quasi-reversible solution electrochemistry with the use of an electron transfer promoter, 4,4 bipyridyl

(viologen).[8] At this interface, viologen mediates the electrode surface and protein to promote electron transfer between the pair.   The initial study also pointed to a fundamental property; horse heart cytochrome-c's electron transfer could not be measured at a bare gold surface. This complication is due to protein adsorption which is followed by the denaturing of the protein on the gold surface. However, the electron promoter allowed cyt-c to remain in solution and, as such, its behavior mirrors that of typical solution electrochemistry.

Taniguchi followed Hill and Eddowes with experiments showing the same quasi-reversible behavior using bis(4-pyridyl) disulfide adsorbed to the gold surface.[11] The study bridged the gap between electron mediators and self-assembled monolayers (SAMs) by combining both. More recent work with cyt-c measured the reversible behavior in solution by using -COOH terminated (SAM)[12,13] or DNA[14] on a gold electrode. An alkanethiol SAM is a more stable and well characterized layer, compared to an electron promoter, due to its well-ordered packing.   Bowden and co-workers' study focused on negative charge terminated SAMs because of its attraction to the positively charged cyt-c protein. While the exact orientation of the heme group is unknown, presumably the extra charge will help with favorable alignment. The common thread in these experiments is that blocking the protein from the gold electrode surface is critical to retaining quasi-reversible behavior, but the electron promoters are not necessary to be in the solution, only on the surface of the electrode.

While the primary interests are in solution electrochemistry at gold electrodes, recent focus has moved toward interfacing cyt-c with gold nanoparticles. These new studies have shown encouraging results with protein-nanoparticle interfaces. One such

study has looked at the ability of cyt-c to adsorb onto citrate gold colloids. Jiang *et al.* found that the quantity and conformation of cyt-c on colloids varies greatly with particle size and concentration.[15] For example, a 2-4 nm gold nanoparticle showed about 20 cytochrome-c proteins would be adsorbed using their calculations. While the study did not focus on electron transfer, they did show that cyt-c will couple with gold nanoparticles and can be quantitatively measured. More recently, Srivastava *et al.* looked at –COOH terminated monolayer protected gold clusters coated with cyt-c based on complimentary electrostatics.[16] The cyt-c coating retained its native conformation and created a well-defined surface on the monolayer, showing that coupling to particle surfaces is possible.

Following in Srivastava's footsteps, the nanoparticles used for our conjugation are tiopronin monolayer protected clusters (TMPCs) that bear a –COOH group. Through gold-thiol chemistry, a thiol bearing protecting ligand anchors to the gold core. These nanometer sized particles with their many properties find diverse applications in optics,[17,18] electronics,[19-21] and biosensors.[3] Gold nanoparticles have been shown to move electrons by their ability to charge, hold, and release electrons through quantized double layer charging (QDL)[19] and electron tunneling.[20] This makes them ideal for shuttling electrons from the electrode to the protein and back again. While various synthetic routes exist for the creation of gold MPCs,[22] the modified-Brust method is favored due to its aqueous one-phase synthesis.[23] The Brust method yields stable MPCs that have 3 nm average diameters with a protecting ligand monolayer on the surface. This protecting monolayer allows the MPC to be dried and re-dissolved repeatedly without the MPC undergoing decomposition.

In addition to creating stability, the surface ligand also defines other properties of the nanoparticle and can be exchanged post-synthesis. Ligand place-exchange on gold tiopronin monolayer protected nanoclusters (TMPCs) is a facile, highly characterized process.[24] Place-exchange is thought to involve the displacement of one thiol-linked molecule for another through a S_n2 type reaction.[24] The exchange can be carried out in solution by co-dissolution of nanoparticles with the thiol molecule of interest. With enough time, the ligands in solution and nanoparticles will come to equilibrium and develop an ordered surface. The extent of exchange can be controlled by varying time and the concentration of the incoming ligand. Using this approach, biomolecules like cyt-c can be attached through thiol linkers.[25,26]

Thus far, there have been reported successful electrochemical measurements of cyt-c's electron transfer at a mediated electrode, on SAMs, and on DNA. Also, cyt-c has been interfaced and quantitatively measured on colloidal and monolayer protected gold surfaces. Our method improves upon both these foundation by presenting a technique that should maintain native conformation on an MPC and simultaneously allow electrochemical measurements without the promoter or other electrode surface modifications. This chapter describes a method for covalently attaching cytochrome-c to gold MPCs and measuring the resulting nanocomposite's electrochemical behavior.

Experimental

Materials

N-(2-Mercaptopropionyl)glycine (tiopronin), 2-Iminothiolane hydrochloride (98%) (traut's reagent), sinapinic acid, and boric acid (ACS) were purchased from Sigma. Horse heart cytochrome-c (90%) and 4,4 dipyridyl anhydrous (98%), and sodium borohydride (98%) were purchased from Acros Organics and used without further purification. Sodium phosphate, methanol (ACS), acetic acid (ACS), tris free-base recrystallized, and Whatman carboxymethyl cellulose microgranular cation exchanger were purchased from Fisher Scientific. Gold tetrachloroauric acid was synthesized in house from 99.99% gold shot. Water was purified by an 18 MΩ Solution 2000 water purification system.

Synthesis of Tiopronin Monolayer Protected Nanoclusters

Gold tiopronin MPCs were synthesized according to literature.[23] Briefly, 1 g of tetrachloroauric acid (2.5 mmol) and 1.224 g of tiopronin (7.5 mmol) were added together in 100 mL of a 6:1 methanol/acetic acid mixture. The solution was placed in an ice bath for 20 min. followed by the addition 1.13 g of $NaBH_4$ (25 mmol) in 15 mL of water under rapid stirring, and the solution turned black (Caution: very exothermic!). The resulting black nanoparticle solution was continuously stirred for 30 minutes in the ice bath, and then the solvent was removed under vacuum at 35 ºC. Upon completion, the solution was diluted with DI water to 90 mL, adjusted to pH ~1 with concentrated HCl, and placed into dialysis with water for purification.

Characterization

MPCs were characterized using transmission electron microscopy (TEM), thermogravimetric analysis (TGA), UV-Vis, and ^{1}H NMR. Core size was determined by TEM using a Philips CM20 operating at 200 keV with a magnification of 400 kx. TEM sizing was complimented with UV-Vis analysis on a Varian Cary 100Bio from 300-700 nm. Purity was analyzed using ^{1}H NMR on a Bruker-AV400 to confirm peak broadening
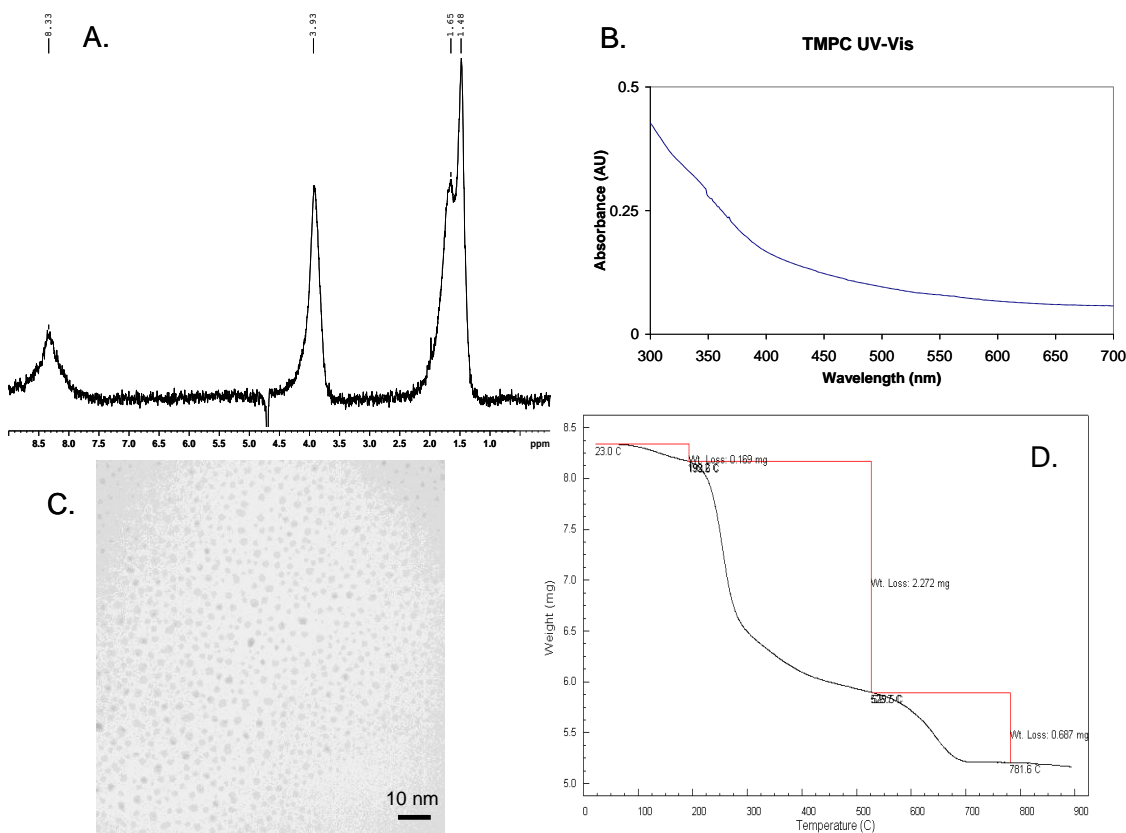

Figure 32. Characterization techniques for the tiopronin monolayer protected clusters. The NMR (A.) shows peak broadening indicative of bound ligands with no impurities from solvents and starting material. The UV-Vis spectra (B.) lacks a surface plasmon peak at 520 nm, which indicates particles sizes less than 5 nm. Also, the UV-Vis shows rayleigh scattering from the solid core starting at 450nm. TEM imaging (C.) has well dispersed single cores with a mean size of 3.6 +/- 1.0 nm. From the TGA (D.), the particles have approximately 28.9% organic coating, based on the initial correction for water's mass at 100 ºC.

indicative of bound ligands.[27] TGA was run from 25-900 °C using an Instrument Specialists TGA 1000 to elucidate the organic percentage, indicating our metal to ligand ratio for composition calculations. Figure 32 shows characterization details from the techniques.

MPC-Cytc-c Conjugation

One μmol of cytochrome-C (12.384 mg) was dissolved in 4 mL of 0.1 M phosphate buffer previously adjusted to pH 7.2. This solution was placed into a plastic reaction vessel, stirred, and sealed with a rubber septum. The cyt-c was purged with
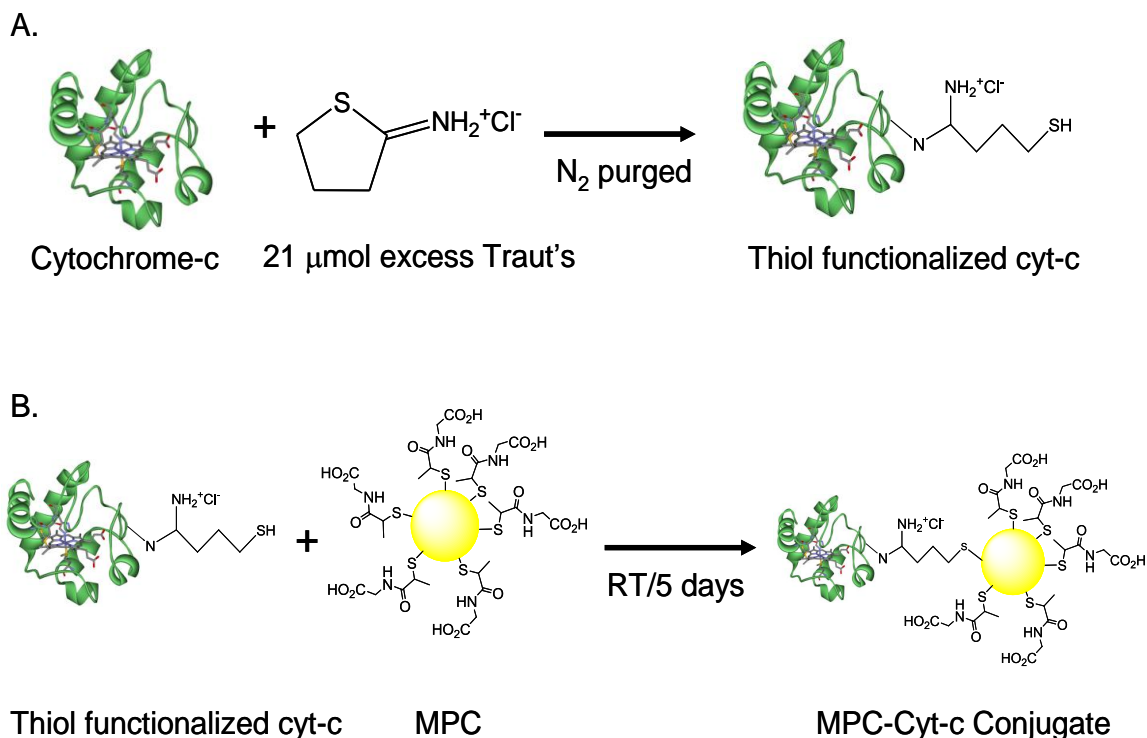

Figure 33. Two step preparation of a protein-MPC conjugate. The first step is the addition of a thiol group followed by the subsequent co-dissolution of the MPC and protein for place-exchange.

nitrogen for 15 minutes to displace dissolved oxygen. Next, 8.64 mg of Traut's reagent (63 μmol) was dissolved in 3 mL of phosphate buffer (Figure 33). From this solution, 1 mL (or 21 μmol) of solution was added to the buffered protein. After injection, nitrogen was bubbled for an additional 45 minutes until the thiolation addition was complete. This sample was then analyzed via MALDI-MS, using a Voyager-DE STR operating at 25 kV, 93% grid voltage, with a mass range of 5200-15000 Da (S2 in supplemental). Samples were made using sinapinic acid as a matrix on a stainless steel plate. After confirming the thiol-functionalization of the cyt-c, 50 mg of MPCs (0.20 μmol) were added to the reaction vessel. The container was sealed under nitrogen and stored in the dark at room temperature for 5 days to allow place exchange.

Separation

Nanoparticle conjugates and free cytochrome-c were separated using an in-house continuous free-flow electrophoresis (CFFE) instrument. The sample was injected into the instrument using a low conductivity tris-borate buffer (20 mM, 500 ᵐˢS/cm, pH 7.5). The sample chamber potential was set to 400 V to perform separation under a constant flow of 1 mL/min. Fractions were collected and tested via UV-Vis from 700-300 nm, with similar fractions being pooled and concentrated for electrochemical testing.

Electrochemical Measurements

All experiments were performed on a CH Instruments electrochemical workstation (CHI660A) with a picoamp booster and Faraday cage. This experiment used

a standard 3-electrode system: a gold working electrode (CHI101, CH Instruments), a 3 M KCl Ag/AgCl reference electrode (CHI1111, CH Instruments), and a platinum mesh counter electrode.

The gold electrode was first mechanically cleaned using 0.2 μm alumina powder and periodically checked for smoothness under a microscope. Next, the electrode was rinsed with water and then sonicated using water followed by ethanol, both for 30 seconds. The electrode was dried under nitrogen and further cleaned electrochemically using 0.5 M sulfuric acid. The electrode was determined clean when the cyclic voltammagram (CV) was reproducible for gold oxide over multiple scans (n = 16).

After cleaning, 4 mL of sample were prepared in PBS for analysis by bubbling argon gas through solution for 30 minutes to remove dissolved oxygen. Afterwards, the argon was flowed above the liquid surface to maintain an inert blanket. CVs were recorded from 250 to –100 mV at scan speeds ranging from 1 to 100 mV/s [9]. In order to boost sensitivity, square wave voltammetry was performed over the same ranges at 1 Hz with a step size of 1 mV/s. Square waves were performed directly following the CV.

The same sample was tested again using a promoted gold electrode. The gold electrode was cleaned as described above and then soaked in a 10 mg/mL aqueous solution of 4,4 dipyridyl for 30 minutes. Experimental order was as previously mentioned, with CVs followed by square wave.

Results and Discussion

Before utilizing these nanoparticles for study, they were first thoroughly characterized. The synthesized nanoparticles had an average diameter of 3.6 ± 1.0 nm

with an organic percentage weight loss of 28.9%. Using this information, the particle's

calculated average composition is $Au_{879}Tiop_{435}$. NMR showed the nanoparticles' purity

by the verification of ligand peak broadening common to nanoparticle ligands and the

lack of any solvent or unbound ligand peaks. After full characterization, the particle was

used for the coupling reaction.

The cyt-c protein was analyzed next to determine the number of thiolated sites

after addition of the Traut's reagent (MW = 137.63g/mole). Characterization of the cyt-c

protein by MALDI-MS revealed a peak shift after thiolation, shown in Figure 34. The

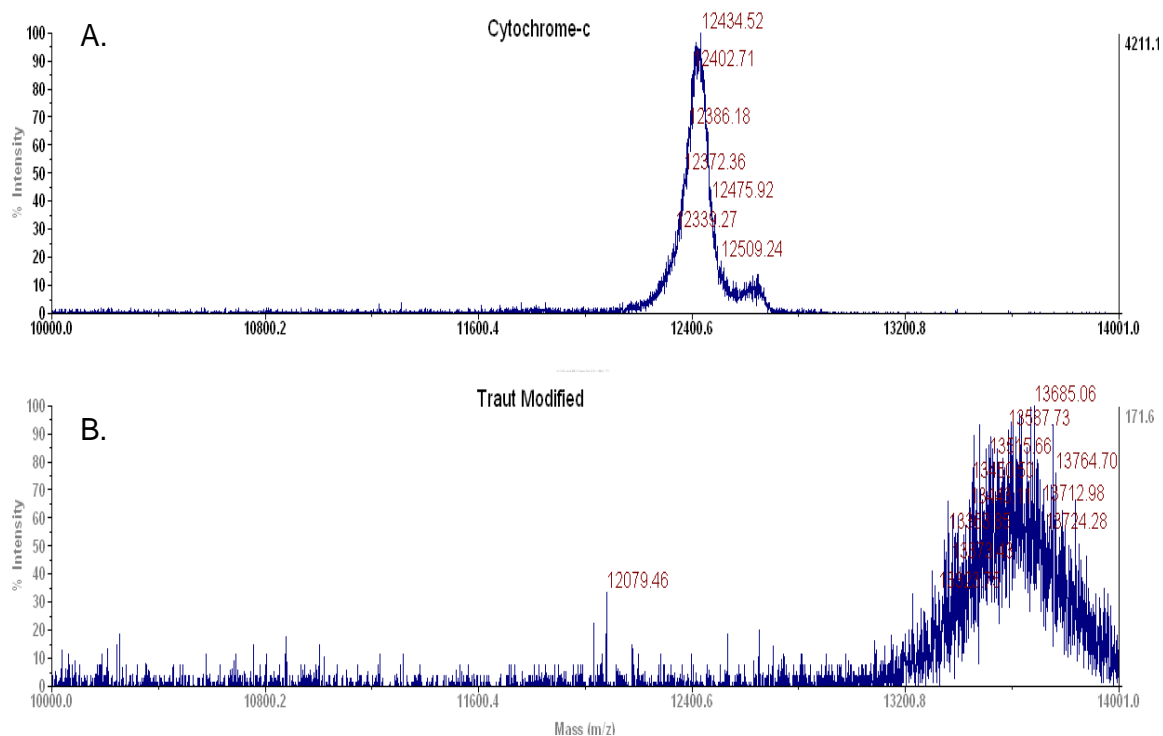shift was from 12.4 kDa to an average peak of 13.6 kDa, which approximates to seven

Figure 34. MALDI-TOF MS spectra of cytochrome-C before (A.) and after (B.) modification with traut's reagent. The modified protein shows a mass shift of 1.2 kDa that converts to seven thiol groups per protein. The intensity of the second spectra is much lower, possibly due to oxidation and dithiol formation between multiple proteins; therefore, making ionization more difficult.

thiolated sites per protein for the coupling reaction. After multiple coupling reactions, any quantity over three sites seemed to give the most viable solution for electrochemical studies.

After synthesizing the protein-MPC conjugate, a continuous free-flow electrophoresis (CFFE) technique was used to rapidly separate coupled particles from the free cyt-c. This was done to remove extraneous signal due to free cyt-c present in solution but not coupled to a nanoparticle. These fractions are then analyzed using UV-Vis to confirm the separation succeeded and to what extent. The fractions in Figure 35 show two different signatures, the continuous scattering of nanoparticles starting at 500 nm and the narrower heme group absorption at 420 nm. Using a 3-D plot, there are divides between free MPCs, coupled MPCs-proteins, and most importantly the free cyt-c. The separation between the free cyt-c and the conjugate is nearly baseline at fraction 36, which allows for confidence that the electrochemical measurements are free of erroneous signal from unbound cyt-c. Both fractions at 33 and 34 were pooled as the MPC-protein conjugates, and fractions 39 and 40 were pooled as free protein.
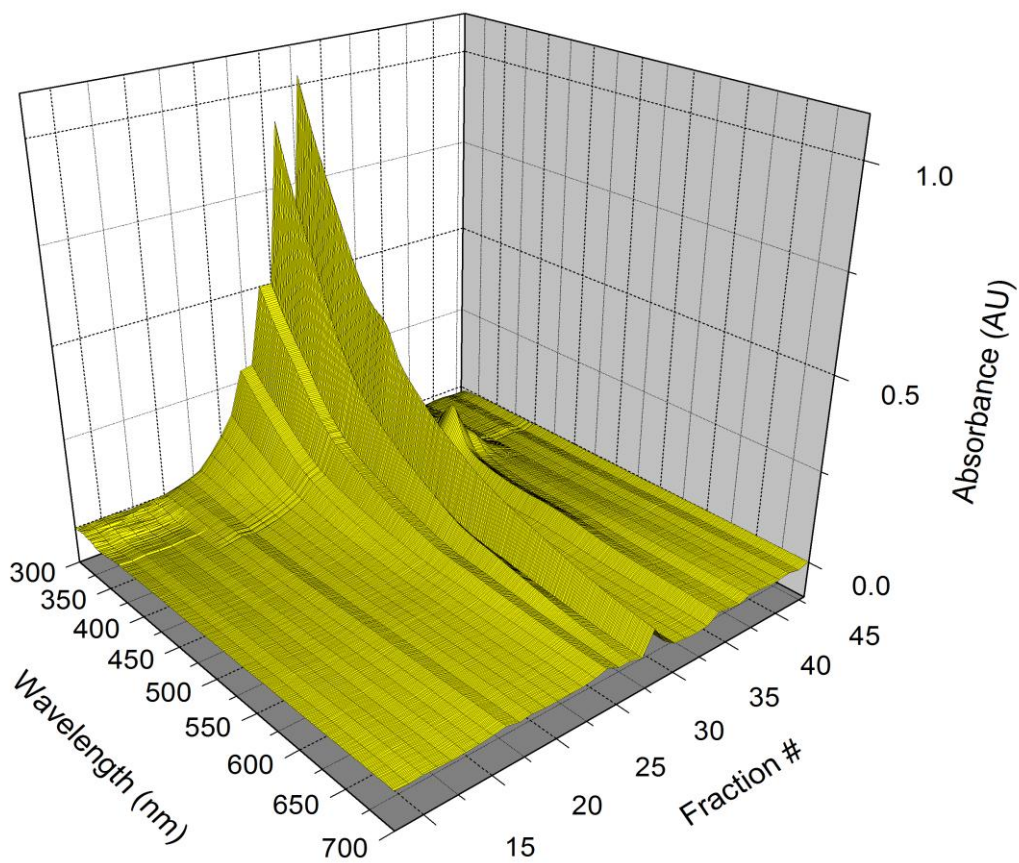
Figure 35: UV-Vis plot of the nanoparticle conjugate separated by CFFE from free cytochrome-c. Fractions 33 and 34 show both characteristics of MPC scattering and cyt-c's 420 nm absorbance. There is near baseline separation around fraction 36, followed by a return of the cyt-c absorbance without MPC scattering at fraction 39. All samples are baseline corrected in relation to fraction 1 (buffer blank).

The initial experiments are focused on cyt-c's behavior before coupling to the nanoparticle, this serves as both a baseline and assurance that the protein is functioning properly. Figure 36 shows the overlaid cyclic voltammograms of the protein with (solid line) and without (dashed line) viologen. The cyt-c shows normal redox behavior with the promoted gold electrode, as can be seen by the reversible behavior (dashed line) instead of the very assymetrical scan without viologen (solid line). The reduction occurs at 45 mV with a current peak (i_p) of 1.215 x 10^{-9} A, while the oxidation peak occurs at E_p of 108 mV with an i_p of -1.862x 10^{-9} A. Both trials were performed at 1 mV/s scan rate
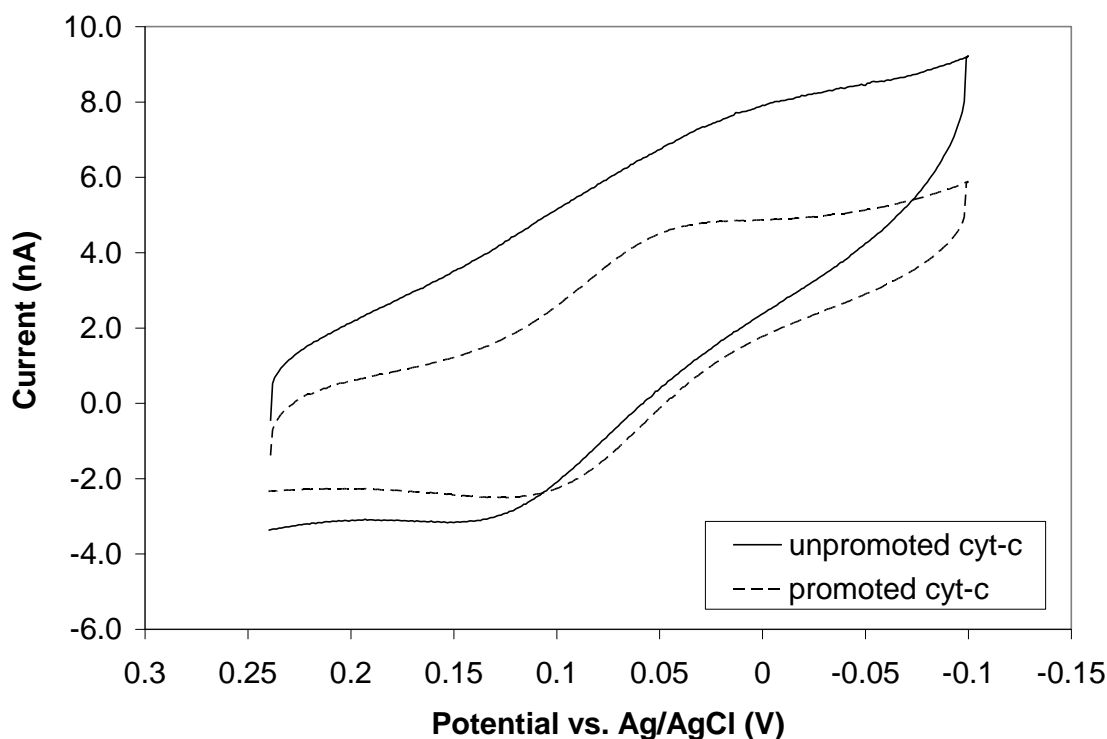

Figure 36. Overlay of two cytochrome-c runs. The solid line is from cyt-c on a bare gold electrode showing the irreversible behavior expected without a mediator. The dashed line with prominent peaks is from the cyt-c on promoted gold. The promoted electrode shows the very reversible behavior associated with cyt-c heme. The scan rate used is 1mV/s.

for consistency. The signal change in the unpromoted, viologen free sample is likely due to the protein denaturing upon adsorption to the gold surface.[7,8] However, like Eddowes and Hill, the addition of viologen to the system helps the protein maintain its native conformation.

After the cyt-c showed typical redox behavior, it was coupled to the nanoparticle using the new thiol bearing groups. The conjugated material shows different behavior with and without the addition of the viologen. Shown in Figure 37 the conjugated material has an i_p of 2.038 x10^{-8} A at E_r of 0.051 mV and of i_p -3.626 x10^{-8} A at E_f of 129 mV. The conjugate actually shows a much higher current compared to the initial cyt-c
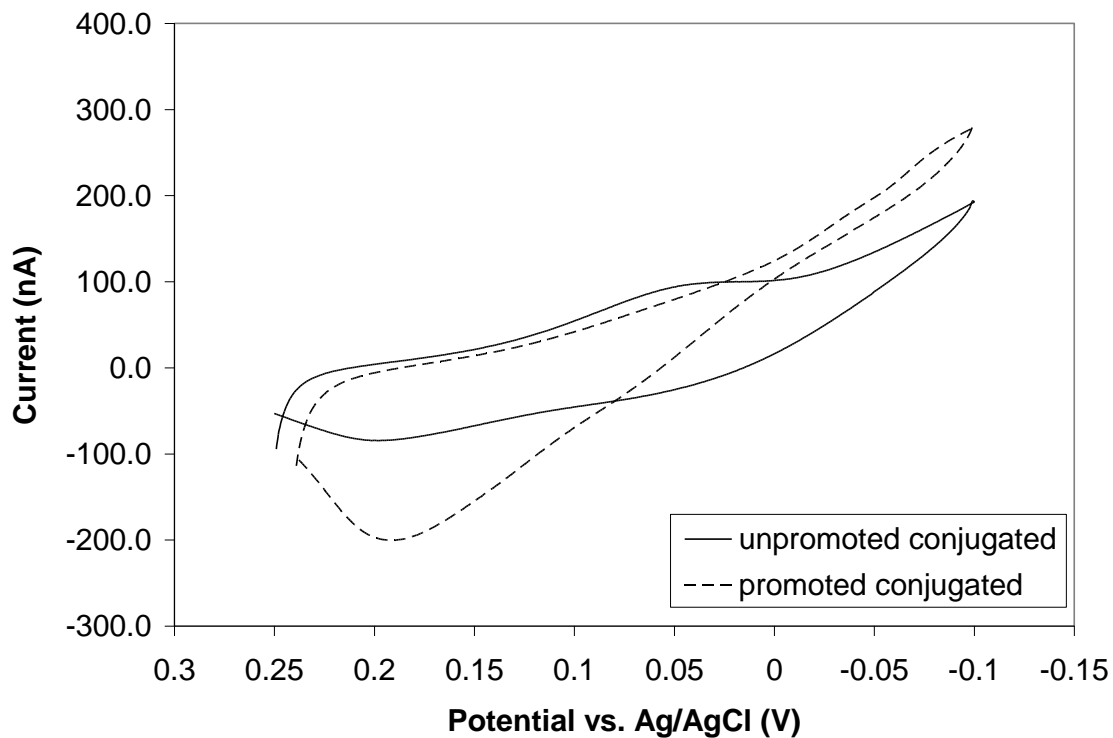
Figure 37: The electrochemical behavior of cytochrome-c conjugated to MPCs. The solid trace is the conjugate without viologen, showing fairly reversible behavior in a mediator free solution. Meanwhile, the dashed line is the same conjugate with viologen added, showing irreversible redox. Both samples were scanned at 1mV/s.

trials. One possibility is that increased concentration of cytochrome-c present on the MPCs leads to more simultaneous electron transfers at the electrode. Also, the peak shifts to a more positive potential, which can be attributed to the attached nanoparticles changing cyt-c's folding, similar to effects noted previously in the literature.[28-31] The voltage shifts vary based on the heme group's solvent exposure. A negative shift indicates overexposure of the heme to solvent and while a positive shift is increased solvent exclusion or increased folding. Another interesting result is the loss of signal with viologen. While normally a promoter, it could be interfering with the electrode and the conjugate, preventing all electron transfer. Another possible explanation is much
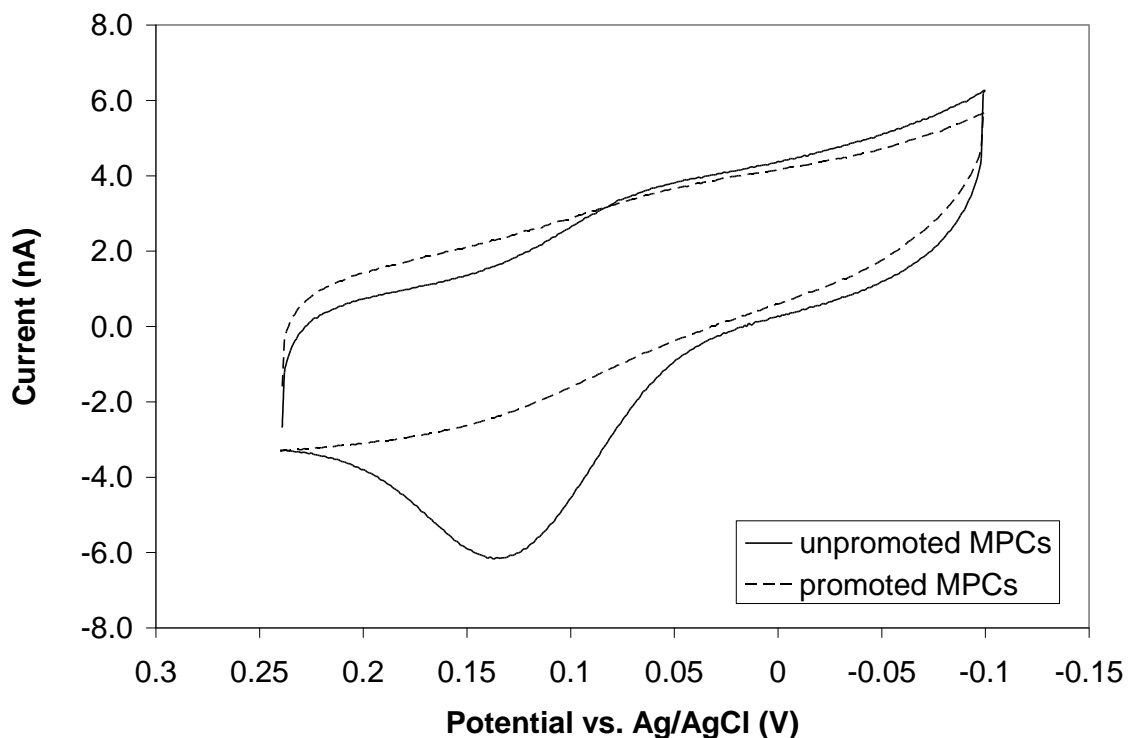

Figure 38. Traces of MPCs in solution. The solid line shows the MPCs from an unconjugated mixture. The dashed line shows the same solution with the addition of the mediator. The promoted scan matches the result seen for the conjugated mixture, with the viologen causing a signal loss. Scans were run at 1mV/s.

slower electron transfer kinetics because of the multiple electron transfer barriers with the conjugate and promoter, compared with protein alone.

As further evidence that only the conjugate is electroactive, a mixture of free MPCs from the separation were analyzed as a control. Figure 38 shows the overlays of both promoted and unpromoted mixtures of MPCs. If any free cyt-c passes concurrently with the MPCs through the CFFE, we would expect to see some signal with the addition of the viologen. The only peaks observed were nearly 100 times less intense than the conjugates, so it can be seen that free MPCs are not active, nor does the CFFE and buffer system impart new electrochemical behaviors. While the promoter blocks the small Au
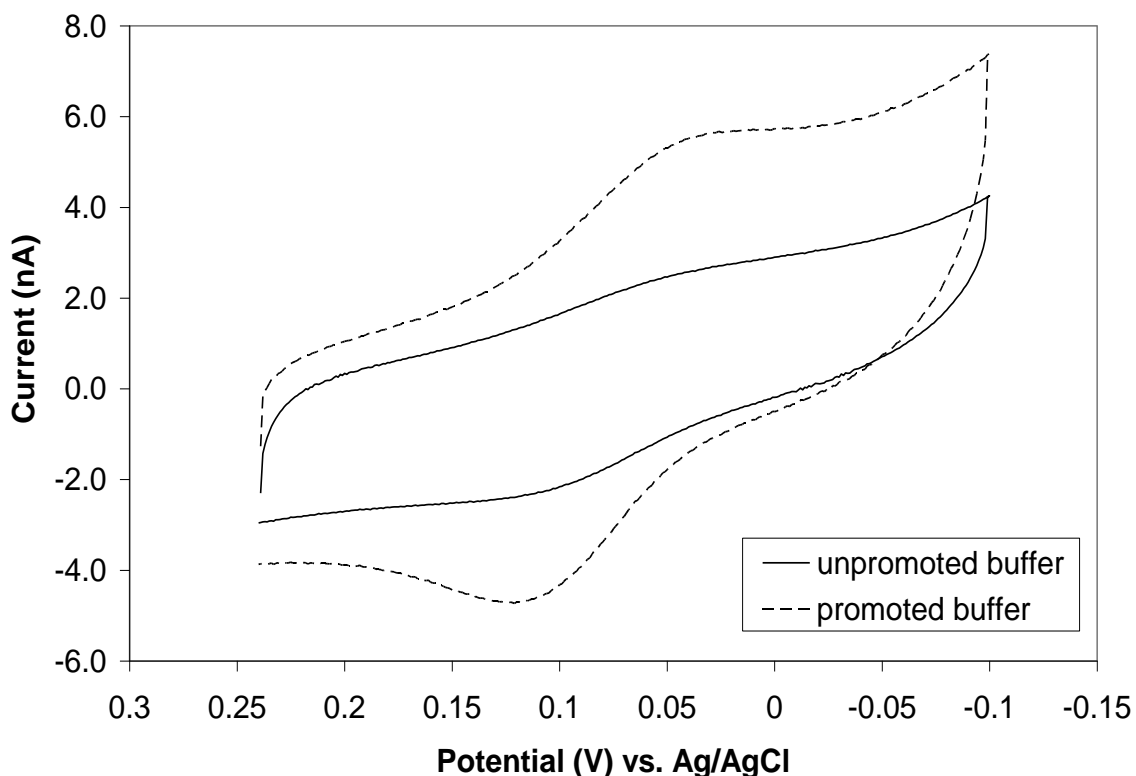

Figure 39. Control run of the buffer solution used in the experiments. Both solutions show minimal redox behavior.

oxide wave, this wave is present in the unpromoted MPCs. In a similar fashion, the buffer shows very little redox chemistry in Figure 39.

Conclusion

We have shown evidence that cytochrome-c's electron transfer to and from an electrode can be facilitated without the use of a promoter or SAM by coupling MPCs directly to the surface of the protein. Our model system uses the redox active cytochrome-c coupled to gold nanoparticles to facilitate electron transfer. With this technique, one could find new proteins to couple with nanoparticles and even tailor certain behaviors or reactions in solution. It is even possible that two different proteins could be used, one as the electron donor, one as the electron acceptor, with the gold particle used as an intermediate for electron transfer. With these new tools, this simple bottom-up engineering scheme has a promising future.

References

(1)   Faulkner, C. J.; Lees, S.; Ciesielski, P. N.; Cliffel, D. E.; Jennings, G. K. *Langmuir* **2008**, *24*, 8409-8412.
(2)   Gerdon, A. E.; Wright, D. W.; Cliffel, D. E. *Anal. Chem.* **2005**, *77*, 304-310.
(3)   Nam, J.-M.; Thaxton, C. S.; Mirkin, C. A. *Science* **2003**, *301*, 1884-1886.
(4)   Noad, R.; Roy, P. *Trends Microbiol.* **2003**, *11*, 438-444.
(5)   Raja, K. S.; Wang, Q.; Finn, M. G. *ChemBioChem.* **2003**, *4*, 1348-1351.
(6)   Blum, A. S.; Soto, C. M.; Wilson, C. D.; Cole, J. D.; Kim, M.; Gnade, B.; Chatterji, A.; Ochoa, W. F.; Tianwei, L.; Johnson, J. E.; Ratna, B. R. *Nano Lett.* **2004**, *4*, 867-870.
(7)   Eddowes, M. J.; Hill, H. A. O. *J.C.S. Chem. Comm.* **1977**, 771-772.
(8)   Eddowes, M. J.; Hill, A. O. *J. Am. Chem. Soc.* **1979**, *101*, 4461-4464.
(9)   Leopold, M. C.; Bowden, E. F. *Langmuir* **2002**, *18*, 2239-2245.
(10)   Nahir, T. M.; Bowden, E. F. *Langmuir* **2002**, *18*, 5283-5286.
(11)   Taniguchi, I.; Toyosawa, K.; Yamaguchi, H.; Yasukouchi, K. *J. Chem. Soc., Chem. Commun.* **1982**, 1032-1033.

(12)   Leopold, M. C.; Black, J. A.; Bowden, E. F. *Langmuir* **2002**, *18*, 978-980.

(13)   Avila, A.; Gregory, B. W.; Niki, K.; Cotton, T. M. *J. Phys. Chem. B* **2000**, *104*, 2759-2766.

(14)   Liu, H. H.; Lu, J. L.; Zhang, M.; Pang, D. W.; Abruna, H. D. *J. Electroanal. Chem.* **2003**, *544*, 93-100.

(15)   Jiang, X.; Jiang, J.; Jin, Y.; Wang, E.; Dong, S. *Biomacromolecules* **2005**, *6*, 46-53.

(16)   Srivastava, S.; Verma, A.; Frankamp, B. L.; Rotello, V. M. *Adv. Mater.* **2005**, *17*, 617-621.

(17)   Schaaff, T. G.; Shafigullin, M. N.; Khoury, J. T.; Vezmar, I.; Whetten, R. L.; Cullen, W. G.; First, P. N.; Gutiérrez-Wing, C.; Ascensio, J.; Jose-Yacamán, M. J. *J. Phys. Chem. B* **1997**, *101*, 7885-7891.

(18)   Alvarez, M. M.; Khoury, J. T.; Schaaff, T. G.; Shafigullin, M. N.; Vezmar, I.; Whetten, R. L. *J. Phys. Chem. B* **1997**, *101*, 3706-3712.

(19)   Cliffel, D. E.; Hicks, J. F.; Templeton, A. C.; Murray, R. W. In *Metal Nanoparticles: Synthesis, Characterization, and Applications.*; Feldheim, D. L., Jr, C. A. F., Eds.; Marcel Dekker, Inc.: New York, 2002, p 297-317.

(20)   Zamborini, F. P.; Leopold, M. C.; Hicks, J. F.; Kulesza, P. J.; Malik, M. A.; Murray, R. W. *J. Am. Chem. Soc.* **2002**, *124*, 8958-8964.

(21)   Laaksonen, T.; Ruiz, V.; Liljeroth, P.; Quinn, B. M. *Chem. Soc. Rev.* **2008**, *37*, 1836-1846.

(22)   Rowe, R. P.; Plass, K. E.; Kim, K.; Kurdak, C.; Zellers, E. T.; Matzger, A. J. *Chem. Mater.* **2004**, *16*, 3513-3517.

(23)   Templeton, A. C.; Chen, S.; Gross, S. M.; Murray, R. W. *Langmuir* **1999**, *15*, 66-76.

(24)   Hostetler, M. J.; Templeton, A. C.; Murray, R. W. *Langmuir* **1999**, *15*, 3782-3789.

(25)   Templeton, A. C.; Cliffel, D. E.; Murray, R. W. *J. Am. Chem. Soc.* **1999**, *121*, 7081-7089.

(26)   Cliffel, D. E.; Zamborini, F. P.; Gross, S.; Murray, R. W. *Langmuir* **2000**, *16*, 9699-9702.

(27)   Templeton, A. C.; Hostetler, M. J.; Warmoth, E. K.; Chen, S.; Hartshorn, C. M.; Krishnamurthy, V. M.; Forbes, M. D. E.; Murray, R. W. *J. Am. Chem. Soc.* **1998**, *120*, 4845-4849.

(28)   Strauss, E.; Thomas, B.; Yau, S.-T. *Langmuir* **2004**, *20*, 8768-8772.

(29)   Stellwagen, E. *Nature* **1978**, *275*, 73-74.

(30)   Kassner, R. J. *Proc. Natl. Acad. Sci.* **1972**, *69*, 2263-2267.

(31)   Tezcan, F. A.; Winkler, J. R.; Gray, H. B. *J. Am. Chem. Soc.* **1998**, *120*, 13383-13388.